

# POROUS SILICON MATRIX FOR APPLICATIONS IN BIOLOGY

Anca Angelescu<sup>1</sup>, Irina Kleps<sup>1</sup>, Miu Mihaela<sup>1</sup>, Monica Simion<sup>1</sup>, Teodora Neghina<sup>1</sup>, Stefana Petrescu<sup>2</sup>, Nicanor Moldovan<sup>3</sup>, Crina Paduraru<sup>2</sup> and Aurelia Raducanu<sup>2</sup>

<sup>1</sup>Institute for Microtechnologies, 32B, Erou Iancu Nicolae Street, R-72296, Bucharest, Romania,

<sup>2</sup> Institute of Biochemistry, 296, Splaiul Independentei Street, sector 6, Bucharest, Romania

<sup>3</sup>The Ohio State University, 310 Davis HLRI, 473 West 12th Avenue, Columbus, Ohio 43210-1252, USA

Received: July 11, 2003

**Abstract.** Different porous silicon (PS) layers, with an average pore size distribution of 10 nm were realised on p+Si (111), and p+Si (100), by partial electrochemical dissolution in hydrofluoric acid based solutions. Various treatments for structure surface modification/stabilisation were made in order to ensure the PS biocompatibility: thermal treatments, carbon layers deposition; hexametildisilazane treatments, and a-SiC deposited by hexametildisilane. On these structures, human retinal endothelial cells (HREC), mouse aortic endothelial cells (MAEC), murine melanomas (B16 – F1), neuronal mouse cells (B50) and hamster ovarian cells (CHO) were grown, and studied by Laser Scanning Cytometry (LSC).

## 1. INTRODUCTION

PS has received much attention because of its optical properties, but also for use in applications like chemical and biological sensors. PS, otherwise known as nano-structured silicon has attracted much recent attention because of its biocompatible, bioactive and biodegradable nature. PS offers a surface topography controllable with nm resolution in three dimensions and allows chemical surface modifications.

Biocompatibility is the ability of a material to interface with a natural substance without provoking a natural response. An effective biomaterial must bond to living tissue – in other words, it has to be 'bioactive'. The attachment of bioactive species for biomaterial applications is straightforward. Nonetheless, PS has not been extensively characterized as a material for implantation. Recent promising findings have shown that biodegradable PS can act as a scaffold for bone tissue engineering.

The high surface area architecture of PS has been investigated as a material for light emission in

all-silicon optoelectronic technology. The silicon hydride present on the porous silicon surface are labile, leading to the oxidation and the formation of luminescence-quenching defects. Replacement of the silicon hydride bonds with silicon alkyls ensures great stability to the material. Researchers have begun to explore the porous silicon as a biodegradable material in the field of medicine, for the slow release of drugs/essential trace elements in vivo, and for in vivo diagnostic tests.

Two aspects of porous silicon are of particular relevance for in vivo implants applications: it can be used as a sensitive biosensor for proteins, antigens, and DNA, and it can be modified with a wide range of biological or organic molecules. These two features should allow PS to serve as a versatile biomaterial. Although efforts in this area are still in early developmental stages, combining the biocompatibility of the material with its highly bio-sensitive capabilities should lead to new applications in tissue-based bioassays, drug delivery, and health-monitoring applications.

---

Corresponding author: Anca Angelescu; e-mail: ancaa@imt.ro

## 2. STATE OF THE ART

In 1995, it was shown that by introducing widely varying porosity into Si, its behavior could be tuned from that of a relatively bio-inert material to one that is bioactive, and even resorbable [1]. These in-vitro studies involved immersing various types of material into the simulated body fluids (SBF) for periods of time ranging from hours to weeks. To study the possibility of using porous Si as a substrate for bone growth, it has been shown that PS could induce a precipitation like hydroxyapatite (the mineral phase of bone) on its surface which correlates with in-vivo behavior. Turner and Colicos [2] observed that silicon is receiving increased attention for use as a biomaterial. Crystalline silicon in particular has been used as a textured surface to guide cell alignment, to encapsulate cells for implantation, and as an electroactive substrate to stimulate excitable cells. Morphological behaviour of osteoblasts on silicon, DLC-coated silicon and amorphous C-N film-deposited silicon in organ culture was investigated by C. Du, X.W. Su, F.Z. Cui, X.D. Zhu [3]. They observed that cells on the silicon wafers were able to be attached, but were unable to follow this attachment with spreading. In contrast, the cells attached, spread and proliferated on the DLC coatings and amorphous C-N films without apparent damage of cell physiology. Research in the Sailor group [4] involves the biocompatibility of nanophase materials for applications such as controlled drug release, biomedical implants, artificial organs, and cell-based experimentation platforms. They are developing inorganic materials based on nano-PS that are compatible with live cells for neurobiology and tissue engineering applications. One of the most interesting treatment was a white light promoted hydrosilylation introduced by Buriak *et al.* [5]. They reported that Si-C bonds could be formed on the PS surface even at room temperature using alkenes or alkynes. Three different techniques for this have been demonstrated so far: Lewis acid mediated, white light promoted and cathodic electrografting method [6]. The treated surface is stable even in a boiling solution of alkaline KOH and part of the photoluminescence is preserved. Unfortunately, the efficiency for hydrosilylation reactions is low. For the white light promoted hydrosilylation it is 14%, and even the highest efficiency observed in Lewis acid mediated hydrosilylation is only 28% [7, 8].

Such studies strongly suggest that PS could become an important biomaterial and a versatile interface between the electronic and biological world.

All biomaterials have morphological, chemical and electrical surface characteristics that influence the response of cells to the implant. The initial event is the adsorption of a layer of protein onto the biomaterial. Generally, uncontrolled adsorption of a lot of proteins is undesirable in a biocompatible material.

The absorption of human serum albumin (HSA) and fibrinogen has been measured for PS. Hydration of the porous surface significantly decreases the adsorption of HSA but increases the amount deeper in the porous film. Hydration does not affect the adsorption of fibrinogen, a protein essential in blood clotting processes. The ability to culture mammalian cells directly onto PS, coupled with the material's apparent lack of toxicity, offers exciting possibilities for the future of biologically interfaced sensing. This could involve the development of biologically interfaced neural networks, or electronic sensing with signals being directly sent from a living system to a PS device. Another benefit is that the optical and optoelectronic properties of PS could allow it to be linked to a data logger by optical fibres. This would remove the risk of electromagnetic forces influencing the responses of cells [9]. The main results from literature show that there is a statistically significant correlation of the surface state with biocompatibility, especially with adhesion and proliferation of cells.

## 3. EXPERIMENTAL WORK AND RESULTS

In this paper were developed the following research activities:

- **technologies for different porous silicon (PS) layers with 35-50% porosity** on Si-p+ (100) and Si-p+(111),  $\rho = 0.01-0.018 \Omega\text{cm}$ , followed by different treatments for surface structures modification/stabilisation. Bulk crystalline silicon is rendered porous by partial electrochemical dissolution in hydrofluoric acid based solutions; depending upon the etching conditions, PS has a very complex, anisotropic nanocrystalline architecture of high surface area. The PS surface is hydrophobic, and these treatments lead to the modification of the surface, to become a biomaterial; the PS test structures were characterised by SEM (Fig. 1), TEM and AFM, and the cells grown was emphasized by Laser Scanning Cytometry (LSC).
- **technologies for PS surface modification** in order to ensure its biocompatibility;

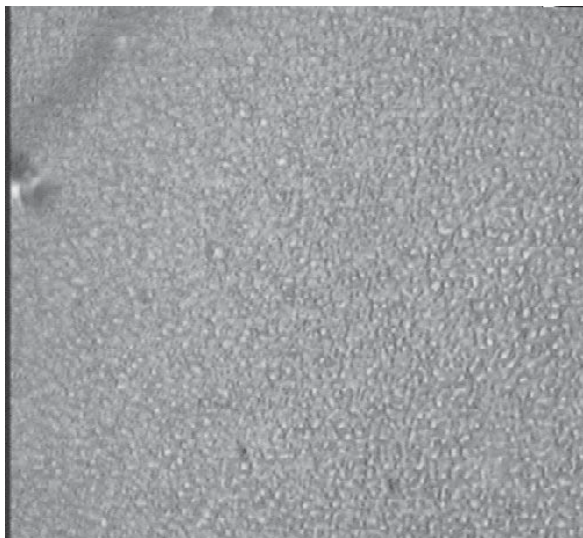


**Fig. 1.** DLC layers on PS substrate obtained from  $\text{CH}_4 + \text{H}_2$  at  $T = 850^\circ\text{C}$ ;  $P = 20$  Torr;  $t_{dep} = 2$  h;  $\text{CH}_4 = 0,015$  l/min;  $\text{H}_2 = 5-6$  l/min; PS (60% porosity, and  $3\mu\text{m}$  thickness) on Si.

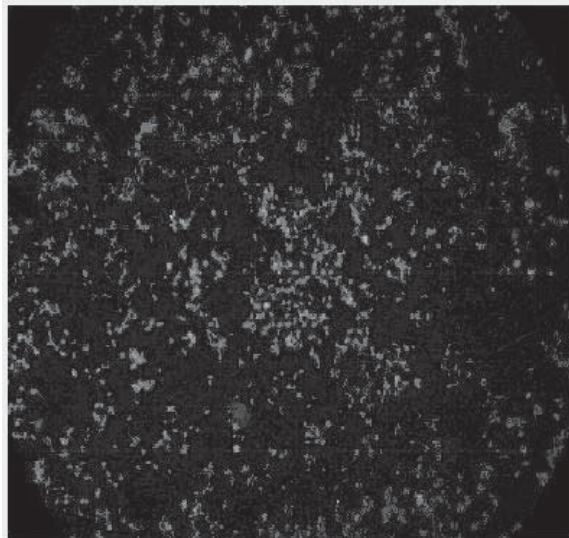


**Fig. 2.** CHO cells on 31 % PS / Sip+ (100), with the surface modified by a 30 nm carbon (10x).

- **study of cell culture growth on the surface of the micro-PS matrix;** on these structures, human retinal endothelial cells (HREC), mouse aortic endothelial cells (MAEC), murine melanomas (B16 – F1), neuronal mouse cells (B50) and hamster ovarian cells (CHO) were grown. HREC and MAEC were grown from different seeding density solutions; the synthesis of the experiments are presented in Tables 1-5: mouse aortic endothelial cells grown on various functionalized PS surfaces, seeding density:  $5 \times 10^4$  cells/cm<sup>2</sup> (Table 1); human retinal endothelial cells (HREC) grown on PS and nanocrystalline silicon oxidized surfaces, seeding density:  $3 \times 10^4$  cells/cm<sup>2</sup> (Table 2) and seeding density:  $1.5 \times 10^4$  cells/cm<sup>2</sup> (Table 4); mouse aortic endothelial cells (MAEC) grown on PS and nanocrystalline silicon oxidized surfaces, seeding density:  $3 \times 10^4$  cells/cm<sup>2</sup> (Table 3) and seeding density:  $1.5 \times 10^4$  cells/cm<sup>2</sup> (Table 5).

#### 4. CHO AND B16-F1 ADHERENCE ON CARBON FUNCTIONALIZED PS

PS biocompatibility can be improved by a suitable change of the surface parameters. There are several possible methods for influencing the roughness and chemical state of the surface. The physico-chemical properties of the surface are controlled by the process technology. Nanocrystalline silicon reacts with the compounds to create a carbon-silicon bond that produces a stabilising coat.

The biocompatibility is determined by two main properties: the normal electrochemical potential and surface energy with respect to the living body. Studies of the electrochemical potential of a number of materials used in medicine have shown that only carbon, gold, and platinum have values close to those of living tissue: +0.330, +0.332, and +0.334 mV, respectively. The surface energy of these elements ranges from 20 to 30 erg/cm<sup>2</sup>, which likewise corresponds to the values for living tissue.

Generally the carbon layer structure is formed by mixed  $\text{sp}^2$  and  $\text{sp}^3$  bonding. The high fraction of the  $\text{sp}^3$  bonds in the structure of the mixed  $\text{sp}^3 + \text{sp}^2$  bonding, exhibits a high hydrophobic surface which is responsible for the cell attachment.

For the biological applications we developed technologies to obtain different PS layers with 35-50% porosity on Si-p+ (100) and Si-p+(111),  $\rho = 0.01 - 0.018 \Omega\text{cm}$ , followed by different treatments for surface structure modification/stabilisation. Different PS surface treatments, like: (i) thermal treatments in  $\text{O}_2$ , (ii) thin carbon, or silicon carbide layer deposition, (iii) thin gold layers, (iv) surface derivatization by an electrochemical method, have been reported to produce a PS hydrophilic and stable; by these treatments the modified surface acquires biomaterial properties.

Previously different carbon layer were deposited on PS structures [10-18]. In Table 1 the technologies used to modify the porous silicon surface in order to ensure its biocompatibility are presented.

**Table 1.** Mouse Aortic Endothelial Cells grown on various functionalized PS surfaces.

Cell Type	Mouse Aortic Endothelial Cells												
Growth Period	24 Hours												
Growth Medium	DMEM (10% FBS, 1% PSA)												
Seeding Density	5·10 <sup>4</sup> cells/cm <sup>2</sup>												
Fixing Medium	100% Ethanol at – 20 °C												
Stain (Nuclear)	Propidium Iodide												
		Wafer	Area of Scan (cm <sup>2</sup> )	# of Cells	Cell Density Cells/cm <sup>2</sup>	Nuclear Area μm <sup>2</sup>	Brightness Max Pixel						
P <sup>+</sup> (111) (branches structure), pores size ~50 nm	Porous silicon native oxidized	0.086	3292	3.8101·10 <sup>4</sup>	139	15149							
20 mA/cm <sup>2</sup> , HF:Et=7:3, 5 min (sample A)	Non-porous silicon native oxidized	0.086	5941	6.9303·10 <sup>4</sup>	169	6170							
P <sup>+</sup> (100) (columnar pores) ~50 nm; 20 mA/cm <sup>2</sup> , HF:Et=7:3, 5 min; carbon monolayer (sample II)	Porous silicon covered by thin carbon	0.086	7234	8.3727·10 <sup>4</sup>	67	2637							
P <sup>+</sup> (100) 20 mA/cm <sup>2</sup> , HF:Et=7:3, 5 min	Non-porous silicon covered by thin carbon	0.086	4989	5.8198·10 <sup>4</sup>	65	2794							
30 nm carbon layer (sample B5)	Porous silicon covered by carbon	0.086	7957	9.2094·10 <sup>4</sup>	139	3994							
P <sup>+</sup> (100); 20 mA/cm <sup>2</sup> , HF:Et=7:3, 5 min oxygen; 300 °C, 30 min. + 800 °C, 60 min (sample B11)	Non-porous silicon covered by carbon	0.086	2637	3.0761·10 <sup>4</sup>	143	4770							
P <sup>+</sup> (100); 20 mA/cm <sup>2</sup> , HF:Et=7:3, 5 min	Porous silicon thermal oxidised	0.086	108	1.25·10 <sup>3</sup>	48	2175							
P <sup>+</sup> (100); 20 mA/cm <sup>2</sup> , HF:Et=7:3, 5 min	Non-porous silicon thermal oxidised	0.086	1125	1.1345·10 <sup>4</sup>	70	1804							
5 min hexamethyldisilazane (sample B20)	Porous silicon methylised	0.086	2390	2.7077·10 <sup>4</sup>	99	2767							
P <sup>+</sup> (100); 100 mA/cm <sup>2</sup> , HF(50%), 5 min; 1 min hexamethyldisilazane (sample B22)	Non-porous silicon methylised	0.086	3824	4.5690·10 <sup>4</sup>	54	10571							
	Porous silicon methylised	0.086	6660	12.3336·10 <sup>4</sup>	192	2957							
	Non-porous silicon methylised	0.086	2733	2.1714·10 <sup>4</sup>	118	11579							

**Table 2.** Human Retinal Endothelial Cells (HREC) grown on PS and nanocrystalline silicon oxidized surfaces. (Seeding Density:  $3 \times 10^4$  cells/cm<sup>2</sup>).

Cell Type:	Human Retinal Endothelial Cells (HREC)					
Growth Medium	DMEM + 10% FBS + 1% PSA					
Seeding Density	3·10 <sup>4</sup> cells/cm <sup>2</sup>					
Fixing Medium	100% EtOH at -20 ° C					
Stain (Nuclear)	Propidium Iodide (PI)					
Growth Surface	Growth Period	# of Cells	Area of Scan (cm <sup>2</sup> )	Cell Density (cells/cm <sup>2</sup> )	Mean Nuclear Area (µm <sup>2</sup> )	Brightness Max Pixel
Oxidized porous Si	24 hours	622	0.086	0.84 E+03	77	4014
Oxidized nanocrystalline silicon	24 hours	167.8	0.086	0.32 E+03	343	6623
Plain Si chip	24 hours	1453	0.086	0.2 E+04	158	4614
Oxidized porous Si	72 hours	1296	0.086	0.3 E+04	153	3822
Oxidized nanocrystalline silicon	72 hours	1749	0.086	0.33 E+04	328	5882
Plain Si chip	72 hours	2911	0.086	0.53 E+04	160	5456

**Table 3.** Mouse Aortic Endothelial Cells (MAEC) grown on PS and nanocrystalline silicon oxidized surfaces. (Seeding Density:  $3 \cdot 10^4$  cells/cm<sup>2</sup>).

Cell Type: Mouse Aortic Endothelial Cells (MAEC)

Growth Medium DMEM + 10% FBS +1% PSA

Seeding Density  $3 \times 10^4$  cells/cm<sup>2</sup>

Fixing Medium 100% EtOH at  $-20^\circ \text{C}$

Stain (Nuclear) Propidium Iodide (PI)

Growth Surface	Growth Period	# of Cells	Area of Scan (cm <sup>2</sup> )	Cell Density (cells/cm <sup>2</sup> )	Mean Nuclear Area (μm <sup>2</sup> )	Brightness Max Pixel
Oxidized porous Si	24 hours	983	0.086	0.28 E+04	301	5498
Oxidized nanocrystalline silicon	24 hours	1032	0.086	0.27 E+04	249	10182
Plain Si chip	24 hours	1254	0.086	0.46 E+04	250	10264
Oxidized porous Si	72 hours	NA	NA	NA	NA	NA
Oxidized nanocrystalline silicon	72 hours	NA	NA	NA	NA	NA
Plain Si chip	72 hours	1300	0.086	0.3 E+04	225	7752

**Table 4.** Human Retinal Endothelial Cells (HREC) grown on PS and nanocrystalline silicon oxidized surfaces. (Seeding Density:  $1.5 \cdot 10^4$  cells/cm<sup>2</sup>).

Human Retinal Endothelial Cells (HREC)

DMEM + 10% FBS +1% PSA

 $1.5 \cdot 10^4$  cells/cm<sup>2</sup>100% EtOH at  $-20^\circ \text{C}$ 

Propidium Iodide (PI)

Growth Surface	Growth Period	# of Cells	Area of Scan (cm <sup>2</sup> )	Cell Density (cells/cm <sup>2</sup> )	Mean Nuclear Area ( $\mu\text{m}^2$ )	Brightness Max Pixel
Oxidized porous Si	24 hours	414	0.086	$2.105 \text{ E}+03$	254	5083
Oxidized nanocrystalline silicon	24 hours	104.6	0.086	$0.264 \text{ E}+03$	220	6728
Plain Si chip	24 hours	214.7	0.086	$1.38 \text{ E}+03$	52	3473
Oxidized porous Si	72 hours	116	0.086	$0.29 \text{ E}+03$	60	2368
Oxidized nanocrystalline silicon	72 hours	910.75	0.086	$0.33 \text{ E}+04$	71	2772
Plain Si chip	72 hours	148	0.086	$0.804 \text{ E}+03$	100	3005

**Table 5.** Mouse Aortic Endothelial Cells (MAEC) grown on PS and nanocrystalline silicon oxidized surfaces. (Seeding Density:  $1.5 \cdot 10^4$  cells/cm<sup>2</sup>).

Mouse Aortic Endothelial Cells (MAEC)  
 DMEM + 10% FBS +1% PSA  
 $1.5 \cdot 10^4$  cells/cm<sup>2</sup>  
 100% EtOH at  $-20^\circ \text{C}$   
 Propidium Iodide (PI)

Growth Surface	Growth Period	# of Cells	Area of Scan (cm <sup>2</sup> )	Cell Density (cells/cm <sup>2</sup> )	Mean Nuclear Area (μm <sup>2</sup> )	Brightness Max Pixel
Oxidized porous Si	24 hours	448	0.086	2.75 E+03	522	6575
Oxidized nanocrystalline silicon	24 hours	NA	NA	NA	NA	NA
Plain Si chip	24 hours	1025	0.086	1.11 E+04	530	5004
Oxidized porous Si	48 hours	7602	0.086	8.28 E+04	263	3645
Oxidized nanocrystalline silicon	48 hours	NA	NA	NA	NA	NA
Plain Si chip	48 hours	4864	0.086	5.30 E+04	261	6124



To demonstrate the biocompatibility of porous silicon covered with different carbon layers we have cultivated B16-F1 mouse melanocytes in normal conditions (at 37 °C in 5% CO<sub>2</sub> atmosphere in RPMI 1640 medium supplemented with 10% fetal calf serum) using these biomaterials as substrates. After 48 hours the cells were visualized by immunofluorescence technique, the chased protein being calnexin, an endoplasmic reticulum resident lectin-like chaperone, present in all eukariotic cells. The technique involves the formation of antigen-primary antibody complex that is visualised using a secondary antibody coupled with a fluorofor. The final complex, including the fluorescently labelled antigen was visualized using a Nikon Eclipse E600W fluorescence microscope. The experimental data show that PS covered with carbon layers is a good biomaterial with no cytotoxicity (Fig. 2). The pattern for calnexin distribution in the cell is normal; in live cells calnexin is seen only in the ER (the more intense dots) but, because of the fluorescent background we can visualize the entire cell. The number of the adherent cells varies among the different PS substrates indicating a variation between the biological properties of the substrates. The same type of substrate prepared on different silicon wafers presents different number of adherent cells; this might be due to the differences in the surface chemistry and topology. Interestingly, melanocytes grown on some PS substrates were found clustered, which is an unusual features for these cells and this may be due to a lack of uniformity of the modified surface. It is also important to emphasize that no further coating with polylysine or collagen was required, which further recommends these materials as suitable bioactive substrate.

## 5. HREC AND MAEC ADHERENCE AND PROLIFERATION ON OXIDIZED POROUS SILICON AND NANOCRYSTALLINE SILICON

The growing of the cells was investigated by Laser Scanning Cytometry (LSC). Laser scanning cytometry synergistically combines and transcends the advantages of Flow Cytometry, Image Analysis, and Automated Fluorescence Microscopy. Like flow cytometry, Laser Scanning Cytometry uses lasers to excite fluorochromes in cellular specimens and detects the fluorescence in discrete wavelengths with multiple photomultiplier tubes (PMT's).

At 24 hours, the HREC adherence on oxidised PS (seeding density:  $3 \cdot 10^4$  cells/cm<sup>2</sup>) was 3.8 times

higher than on oxidized nanocrystalline silicon, while at 72 hours the HREC proliferation was better on oxidized nanocrystalline silicon (Table 2).

The MAEC adherence at 24 hours (seeding density:  $3 \cdot 10^4$  cells/cm<sup>2</sup>) was almost the same on oxidised PS and on oxidized nanocrystalline silicon. At 72 hours the proliferation was excessive, and a saturation of the LSC measurements was observed (NA indicative in Table 3). A very high cell proliferation in both cases, HREC and MAEC was observed in the case of lower seeding density,  $1.5 \cdot 10^4$  cells/cm<sup>2</sup>.

## 6. CONCLUSIONS

The PS substrates are biocompatible materials, appropriate for cultivating adherent cells *in vivo* and without noticeable toxicity. Moreover, morphologically, the melanocytes cultivated on PS are similar with the control cells. It is also important to emphasize that no further coating with polylysine or collagen was required, which further recommends these materials as suitable bioactive substrate.

HREC and MAEC adherence and proliferation are different depending on silicon surface and on seeding density.

## ACKNOWLEDGEMENTS

The authors would like to thank Dr J.M.Albella, ICM Madrid and Dr I.Stamatin, University of Bucharest for carbon layer deposition; this work was part of the Romanian MATNANTECH National Programms; some experiments were performed in collaboration with Ohio State University, Columbus.

## REFERENCES

- [1] L.T. Canham, *Properties of Porous Silicon EMIS Dataview Series*, No. 18 (INSPEC Publication, London, UK, 1997).
- [2] S. Turner, L. Kam, M. Isaacson, H. G. Craighead, W. Shain and J. Turner // *J. Vac. Sci. Technol. B* **15** (1997) 2848.
- [3] C. Du, X.W. Su, F.Z. Cui and X.D. XD // *Biomaterials* **19** (1998) 651.
- [4] Michael J. Sailor and Y.Y. Li // *Science* **299** (2003) 2045.
- [5] M. P. Stewart and J.M. Buriak // *Angew. Chem. Int.* **37** (1998) 3257.
- [6] E.G. Robins, M.P. Stewart and J.M. Buriak // *Chem Commun.* **24** (1999) 2479.
- [7] M. P. Stewart and J. M. Buriak // *Advanced Materials* **12** (2000) 859.

- [8] M.P. Stewart, E.G. Robins, T.G. Geders, M.J. Allen, H.C. Choi, J.M. Buriak // *Phys. Stat. Sol. (a)* **182** (2000) 109.
- [9] Lorraine Buckberry and Sue Bayliss // *Materials World*. **7** (1999) 213.
- [10] I. Kleps, M. Badila, A. Paunescu and G. Banoiu, In: Proc. of the 9th International Colloquium on Plasma Processes, (Juan-les-Pins, France, June 7-11, 1993).
- [11] I. Kleps, F. Caccavale, G. Brusatin, A. Angelescu and L. Armelao // *Vacuum* **46** (1995) 979.
- [12] I. Kleps and A. Angelescu // *J. Phys. IV* **9** (1999) 1115.
- [13] I. Kleps and A. Angelescu // *Surface Science* **482-485** (2001) 771.
- [14] I. Kleps, A. Angelescu, N. Samfirescu, A. Gil and A. Correia // *Solid-State Electronics* **45** (2001) 997.
- [15] I. Kleps and A. Angelescu // *Applied Surface Science* **184** (2001) 107.
- [16] I. Kleps, D. Nicolaescu, I. Stamatina, A. Correia, A. Gil and A. Zlatkin // *Applied Surface Science* **145** (2002) 152.
- [17] A. Angelescu, I. Kleps, M. Miu, M. Simion, S. Petrescu, A. Raducanu and C. Paduraru, In: *Proc. of MATNANTECH Conference* (Sinaia, Dec. 13-15, 2002).
- [18] Mihaela Miu, Anca Angelescu, Irina Kleps, Monica Simion, Adina Bragaru, Teodora Neghina, Mircea Modreanu, Daniela Iacopino and Paul Roseingrave // *Proceedings of CAS* **99** (2003) 120.